Electronic Supplementary Information (ESI) for

Engineering linker defects in functionalized UiO-66 MOF nanoparticles for oil-in-water Pickering emulsion stabilization

Mostakim SK[±], Salini Kar[±], Jayant K Dewangan and Mithun Chowdhury*

Lab of Soft Interfaces, Department of Metallurgical Engineering & Materials Science,
Indian Institute Technology Bombay, Mumbai 400076, India

* To whom correspondence should be addressed: MC, E-mail: mithunc@iitb.ac.in

[±]Contributed equally (MSK, SK)

Material and methods

All the chemicals and organic solvents, $ZrOCl_2 \cdot 8H_2O$ (99.8 % Loba Chemie), Palmitic acid (99.5 %, Loba Chemie), DMF (99.5 % Loba Chemie), n-heptane (99.9 %, Loba Chemie), Methanol (99.9 %, HPLC, Loba Chemie), terephthalic acid (99.5 %, Loba Chemie), glacial acetic acid (99.8 % Loba Chemie), and $CHCl_3$ (99.9 %, Loba Chemie), were collected from the near chemical supplier and used as received. The organic solvents were used carefully.

The phase purity of the **UP** and **UM** was investigated using an X-ray powder diffraction (XRPD) measurement, PANalytical Empyrean instrument utilizing Cu Kα radiation (λ = 1.54184 Å) from 5 to 50°. The FT-IR (Fourier transform infrared spectra) spectra of all compounds were recorded in the range 450-4000 cm^{-1} by Perkin Elmer FT-IR spectrometer to verify the spectral changes. The thermal stability of **UP '** and **UM'** was measured under N_2 flow using an SDT Q600 V20.9 Build 20 in the temperature range of 25-700 °C. The proton ^{1}H-NMR of the digest compounds in HF-DMSO-d_6 was conducted by a Bruker 500 MHz. The BET surface area of all compounds was determined using a Quantachrome Autosorb iQMP gas sorption analyzer at -196 °C. The water-air contact angles were taken using a contact-angle goniometer (Dataphysics, model OCA15SEC). The homogeneous Pickering emulsion was made by a High Torque Stirrer mixture, model BDC6015, Caframo, USA. The microscopic images were collected by an Olympus BX53M microscope. The solid, stable emulsion droplets were viewed using a scanning electron microscope (SEM) (Hitachi S-3400N). A cryo high-resolution transmission electron microscope (HRTEM) (JEOL, JEM 2100) instrument was used to analyze the emulsion. The TEM images of MOF and emulsion droplets were collected using a TEM instrument (Thermo Scientific, Themis 300 G3). The elemental analysis of MOF and emulsion droplet was measured using a FESEM instrument (JEOL-JSM7600F). All the rheological studies were investigated by an Anton Paar Rheometer (model: Physica MCR702) with a parallel plate measuring system (PPMS) at ambient temperature. The zeta potential of all compounds was determined using a Zetasizer Nano ZS90 (model no. ZEN3690) instrument. The yield of the synthesized MOFs was calculated according to the following procedure outlined at the end of this ESI.[a] The AC electrical conductivity of the Pickering emulsions stabilized by **UP'** was measured using a broadband dielectric spectrometer (Novocontrol Technologies, Germany, Concept 80) with an Alpha A analyzer at room temperature. The measurements were conducted within a frequency range of 10^{-1} to 10^8 Hz.

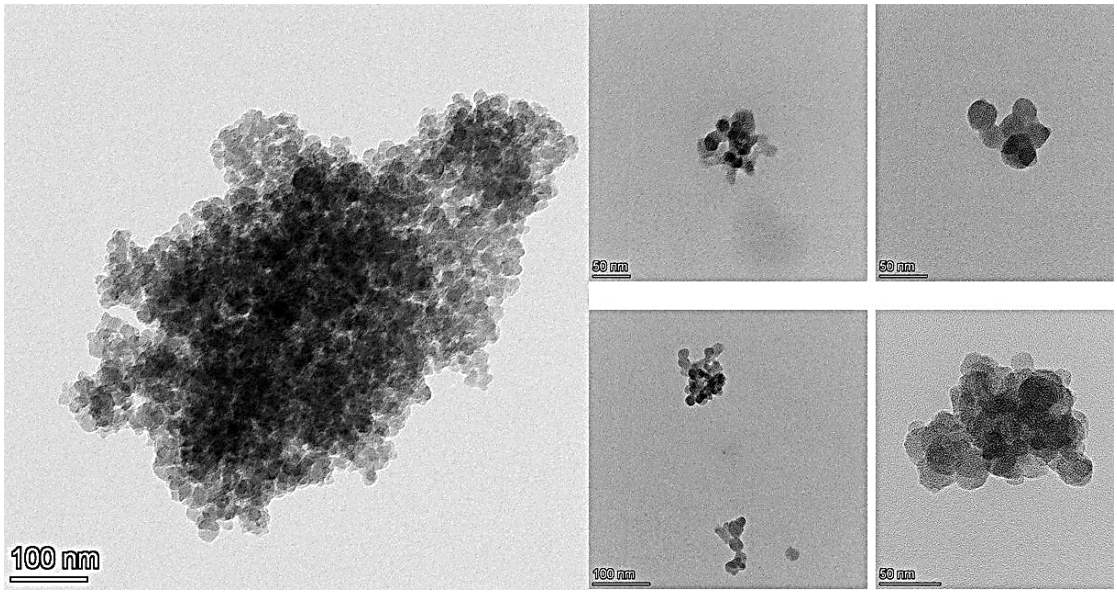

Figure S1. TEM images of **UP'**.

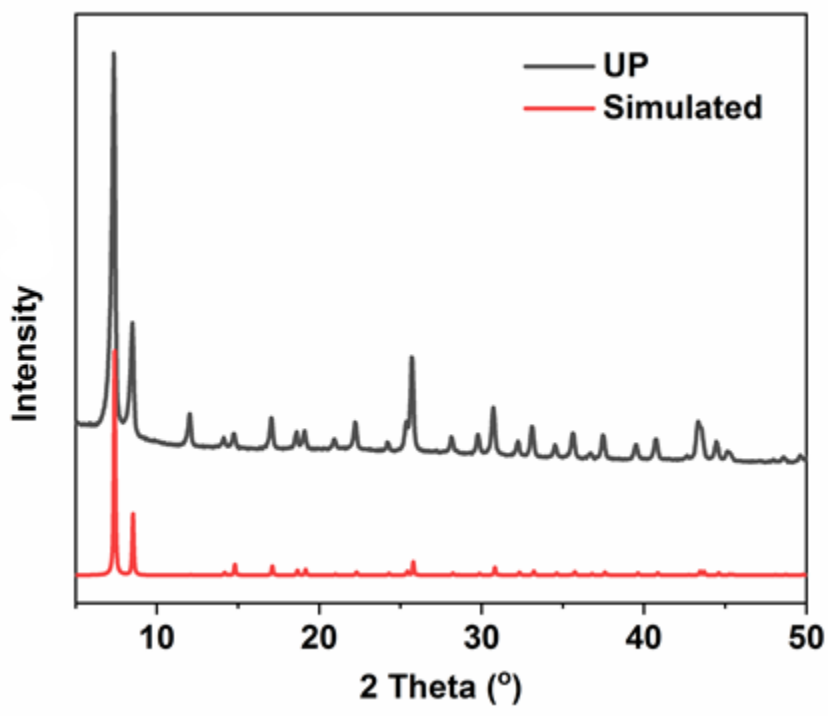

Figure S2. Comparison of PXRD pattern of both as-synthesized (**UP**) and simulated PXRD of UiO-66 MOF. The simulated PXRD data were collected from the previous literature[1].

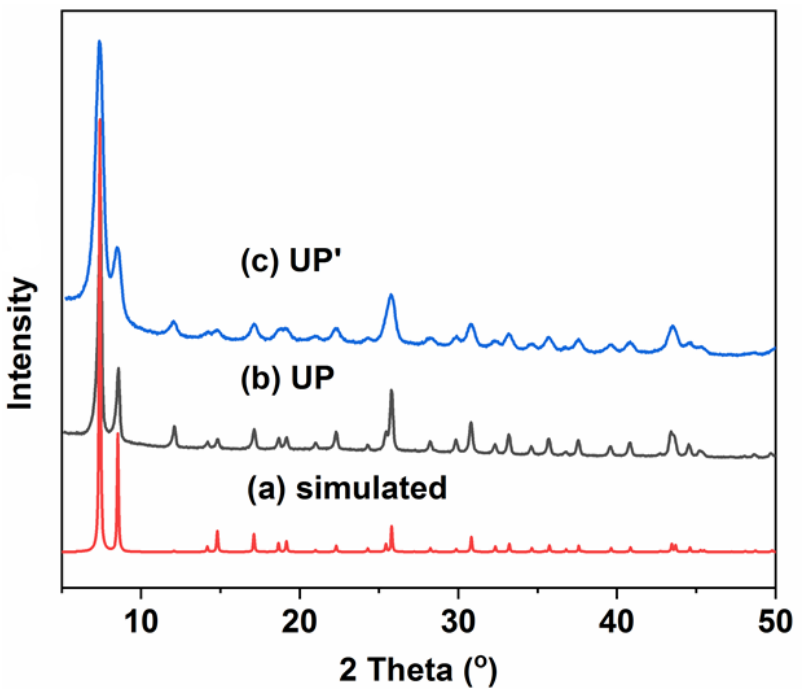

Figure S3. PXRD patterns in different forms: (a) simulated PXRD[1]; (b) as-synthesized (**UP**); (c) activated (**UP'**).

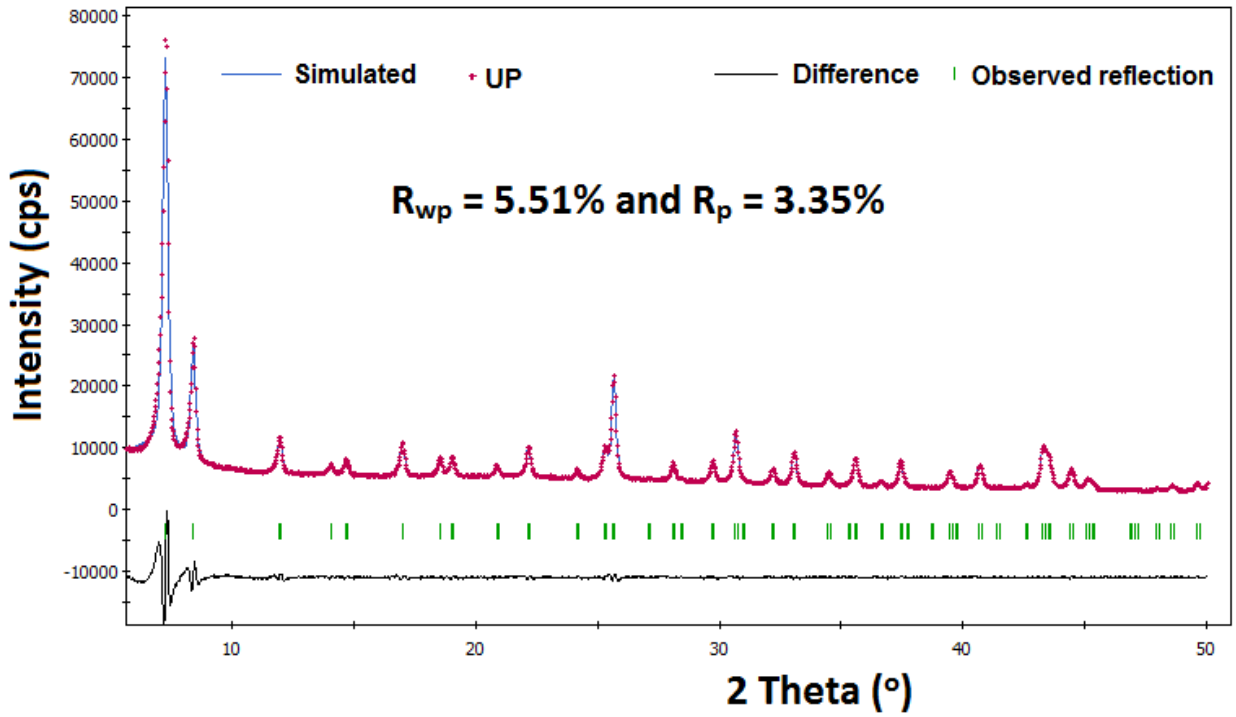

Figure S4. Pawley refinement of the as-synthesized **UP**. Red dots and blue lines denote observed and calculated patterns, respectively. The peak position and difference plot are displayed at the bottom (R_p = 3.35%, R_{wp} = 5.51).

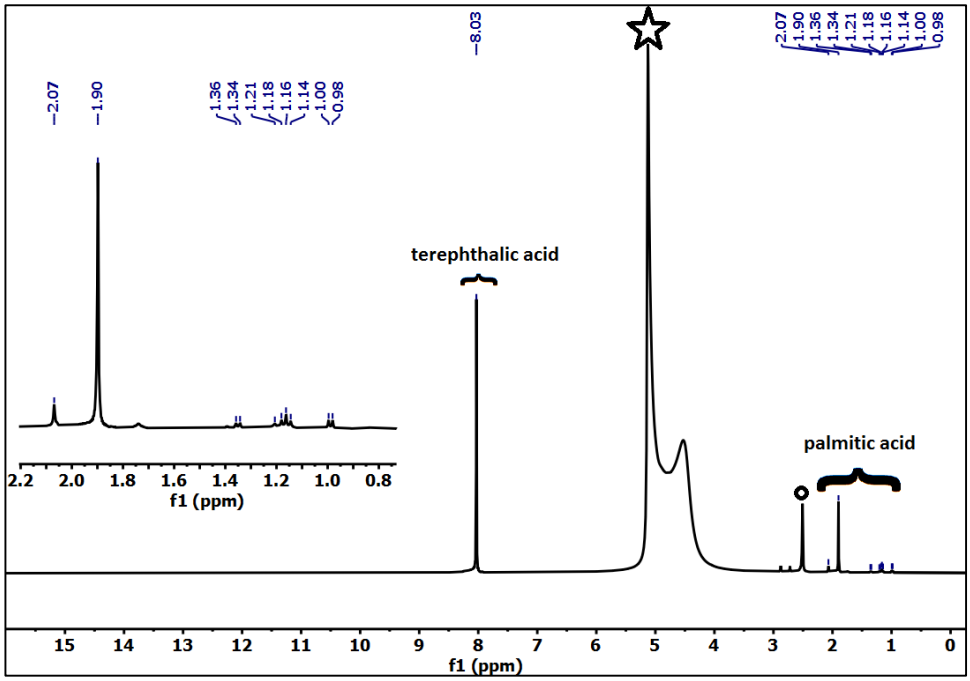

Figure S5. ^{1}H NMR spectra of **UP'** after digestion in HF/DMSO-d_6. The star represents the HF-H_2O, and the circle denotes DMSO-d_6, respectively.

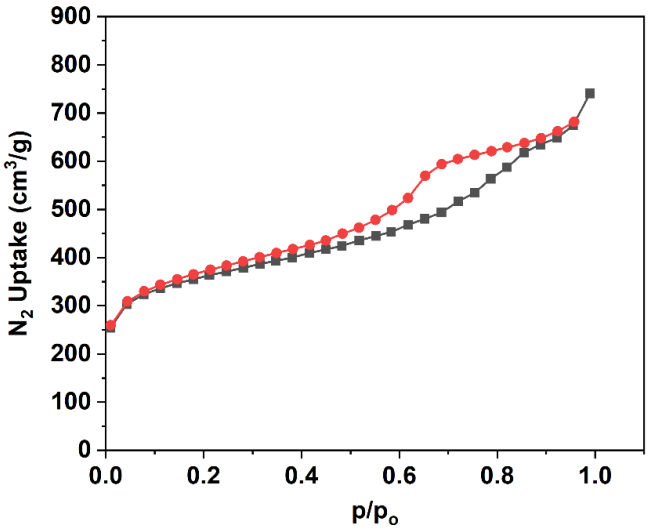

Figure S6. N_2 sorption isotherm of **UM'** at -196 °C.

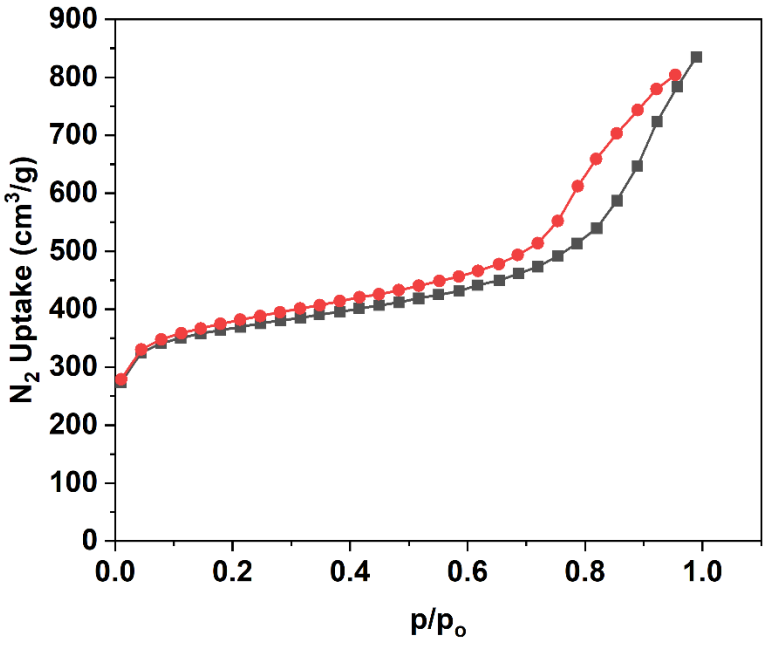

Figure S7. N_2 sorption isotherm of **UP'** at -196 °C.

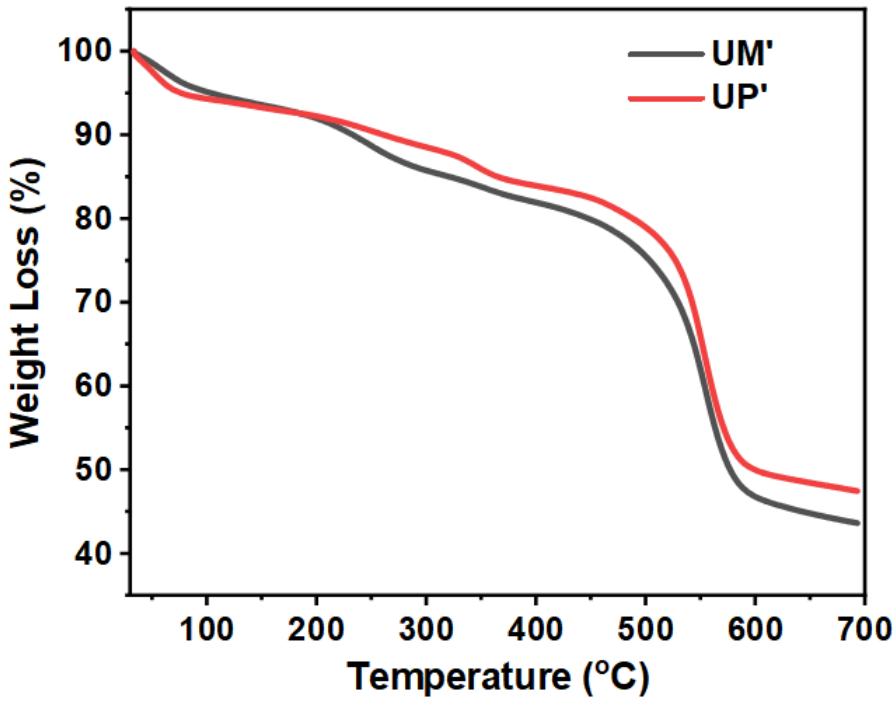

Figure S8. TGA scan of both activated **UP'** (red) and **UM'** (black) compounds measured under N_2 atmosphere (flow rate = 100 ml/min) with a heating rate of 5 °C/ min.

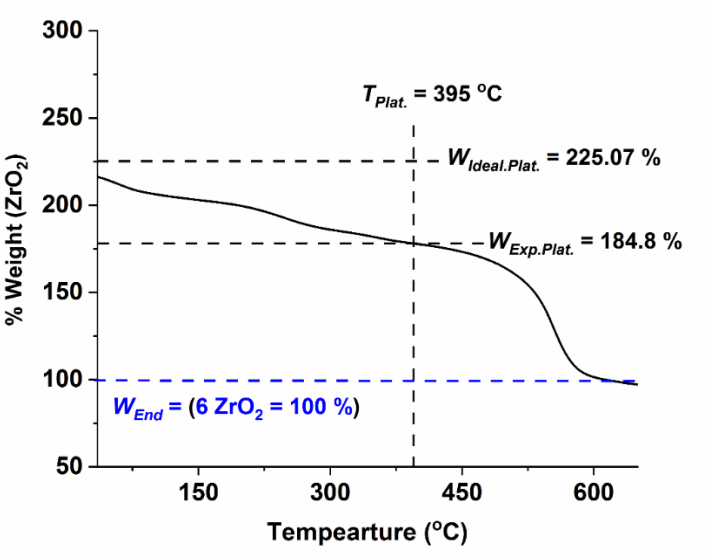

Figure S9. The solid curve is the TGA curve of **UM'** compound. Y-axis is normalized such that the end weight ($\mathbf{W_{End}}$) = 100 %. The vertical dashes line denotes $\mathbf{T_{Plat.}}$ (395 °C), the temperature at which the plateau ($\mathbf{W_{Exp.Plat.}}$ = 184.8 %) is reached. The ideal TGA plateau of **UM'** (without defects) is denoted by $\mathbf{W_{Ideal.Plat.}}$ = 225.07 %. The linker defects were found to be ~1.8. The defect was calculated according to the previous literature.[2]

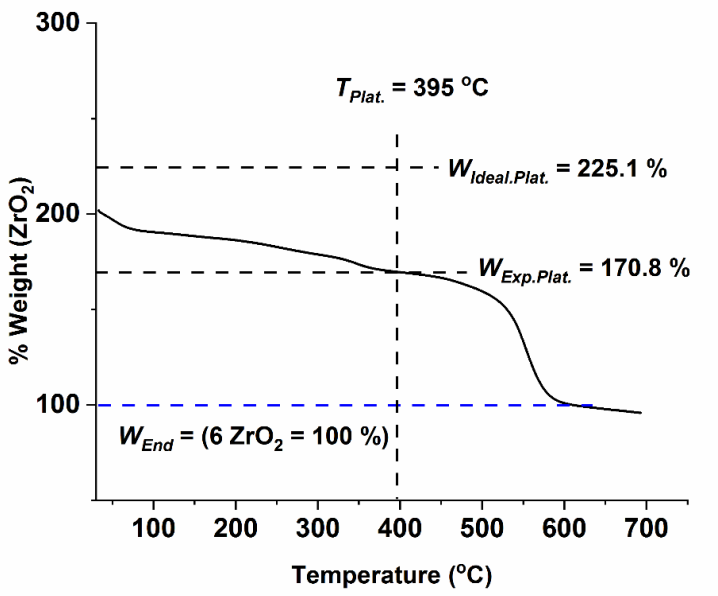

Figure S10. TGA scan of **UP'** compound (solid-curve), Y-axis is normalized such that the end weight ($\mathbf{W_{End}}$) = 100 %. The vertical dashes line denotes $\mathbf{T_{Plat.}}$, (395 °C) the temperature at which the plateau ($\mathbf{W_{Exp.Plat.}}$ = 170.8 %) is reached. The ideal TGA plateau of **UP'** (without defects) is denoted by $\mathbf{W_{Ideal.Plat.}}$ = 225.1 %. The linker defects were found to be ~2.5. The defect was calculated according to the previous literature.[2]

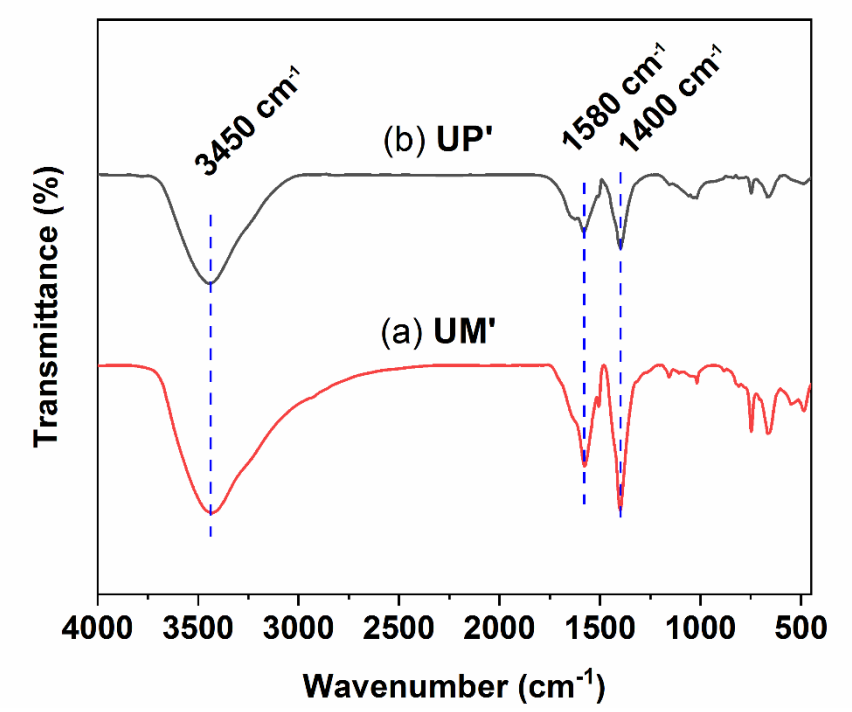

Figure S11. FT-IR spectra of **UP'** (black) and **UM'** (red) compounds.

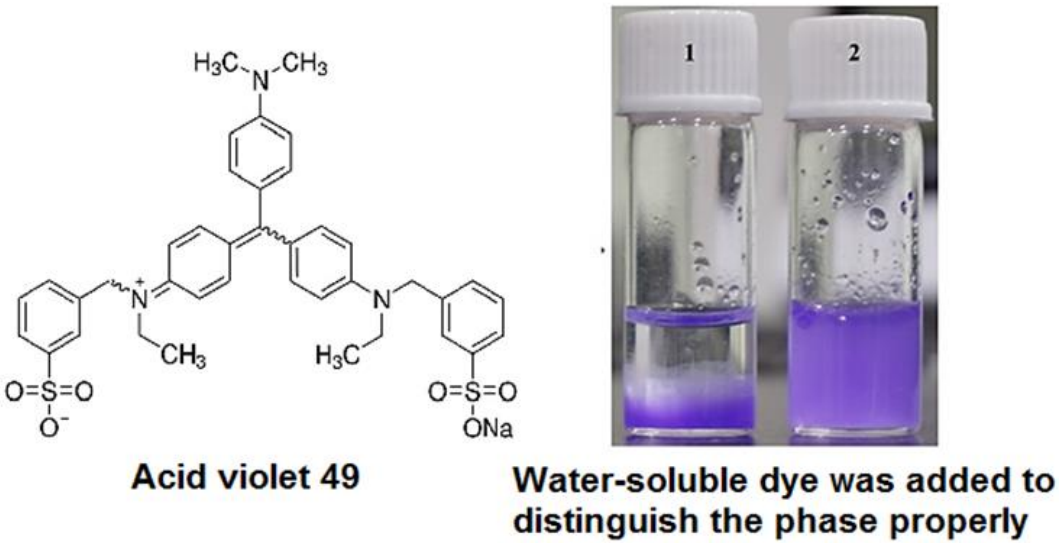

Figure S12. Water-soluble dye (Acid violet 49) was added to distinguish the emulsion phases properly. Vial 1 is an emulsion of **UP'** (**UP'** concentration 8.33 mg/ml) dyed with Acid violet 49, and when heptane is added, that remains separated. In vial 2, dyed emulsion diluted with water gives a well-mixed phase proving the emulsion has water in the continuous phase.

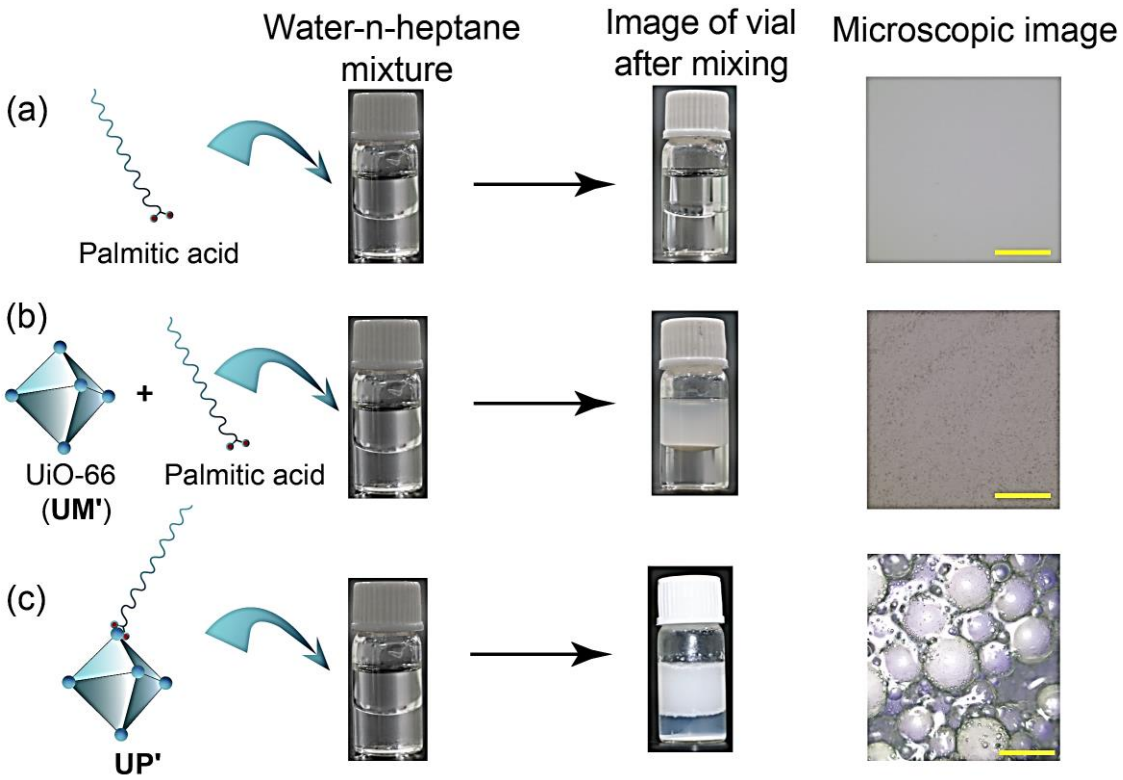

Figure S13. Stabilization of Pickering emulsions using different mixtures; (a) Palmitic acid (4 mg, 0.015 mmol) in water and n-heptane mixture. (b) **UM'** (25 mg, 0.015 mmol) and palmitic acid (4 mg, 0.015 mmol) mixture in water and n-heptane. (c) **UP'** (**UP'** concentration 8.33 mg/ml) in water and n-heptane mixture. Scale bar in each optical micrograph 50 µm.

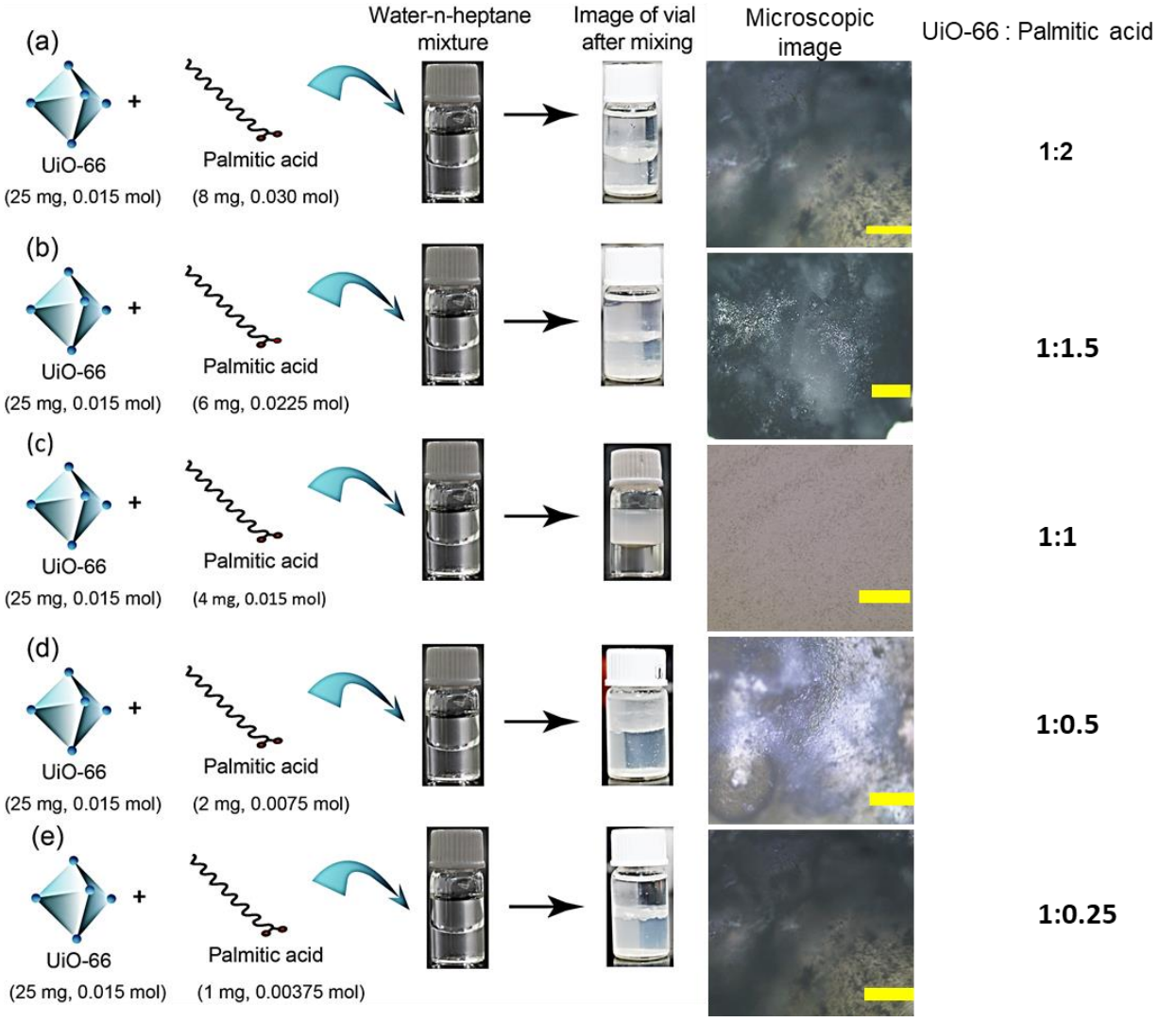

Figure S14. Stabilization of Pickering emulsions by using **UM' (**UiO-66) with different content of palmitic acid; (a) **UM'** (25 mg, 0.015 mmol) and palmitic acid (8 mg, 0.030 mmol) mixture in water and n-heptane mixture. (b) **UM'** (25 mg, 0.015 mmol) and palmitic acid (6 mg, 0.0225 mmol) mixture in water and n-heptane mixture. (c) **UM'** (25 mg, 0.015 mmol) and palmitic acid (4 mg, 0.015 mmol) mixture in water and n-heptane mixture. (d) **UM'** (25 mg, 0.015 mmol) and palmitic acid (2 mg, 0.0075 mmol) mixture in water and n-heptane mixture. (e) **UM'** (25 mg, 0.015 mmol) and palmitic acid (1 mg, 0.00375 mmol) mixture in water and n-heptane mixture. Scale bar in each optical micrograph = 200 µm.

Figure S15. (a) Pickering emulsions of n-heptane-in-water stabilized by **UP'** MOF particles using Acid violet 49 dye. (b) Stabilized Pickering emulsions of n-heptane-in-water using Trypan blue dye. (c) Stabilized Pickering emulsions of n-heptane-in-water using Colcon dye. (Concentration of each water-soluble dye is 0.35×10^{-3} M).

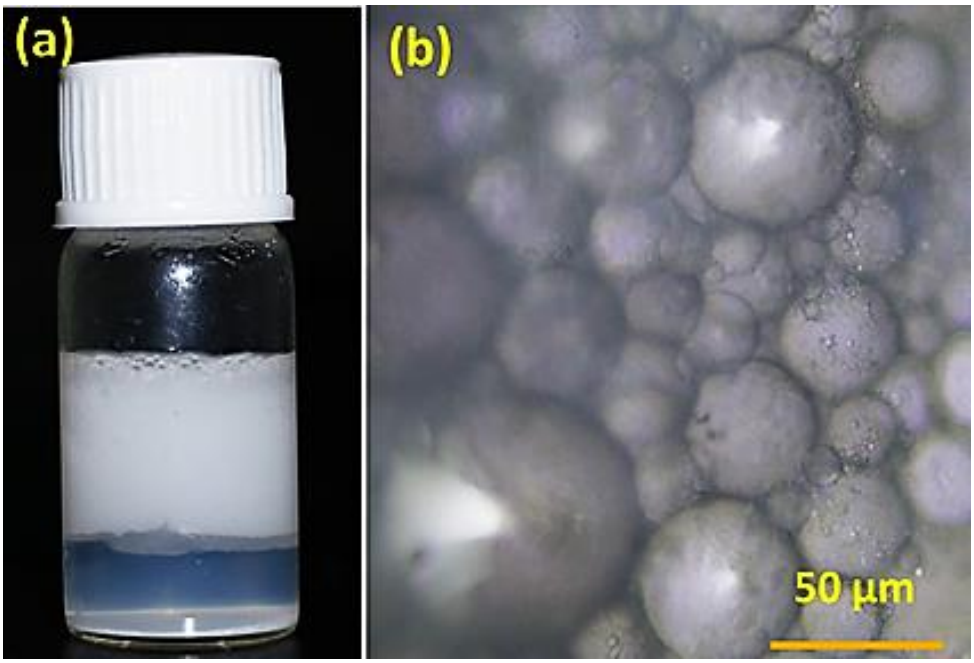

Figure S16. (a) Photographic image of Pickering emulsion stabilized by 25 mg **UP'** after one month. (b) Optical microscopic image of emulsion droplets as shown in (a).

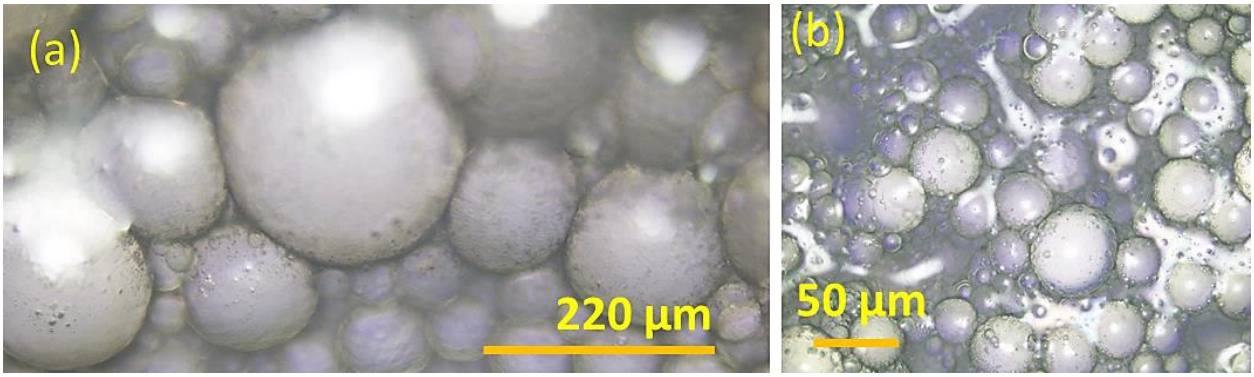

Figure S17. Optical microscopic images of Pickering emulsion stabilized by different content of **UP'**: (a) 5 mg; (b) 25 mg.

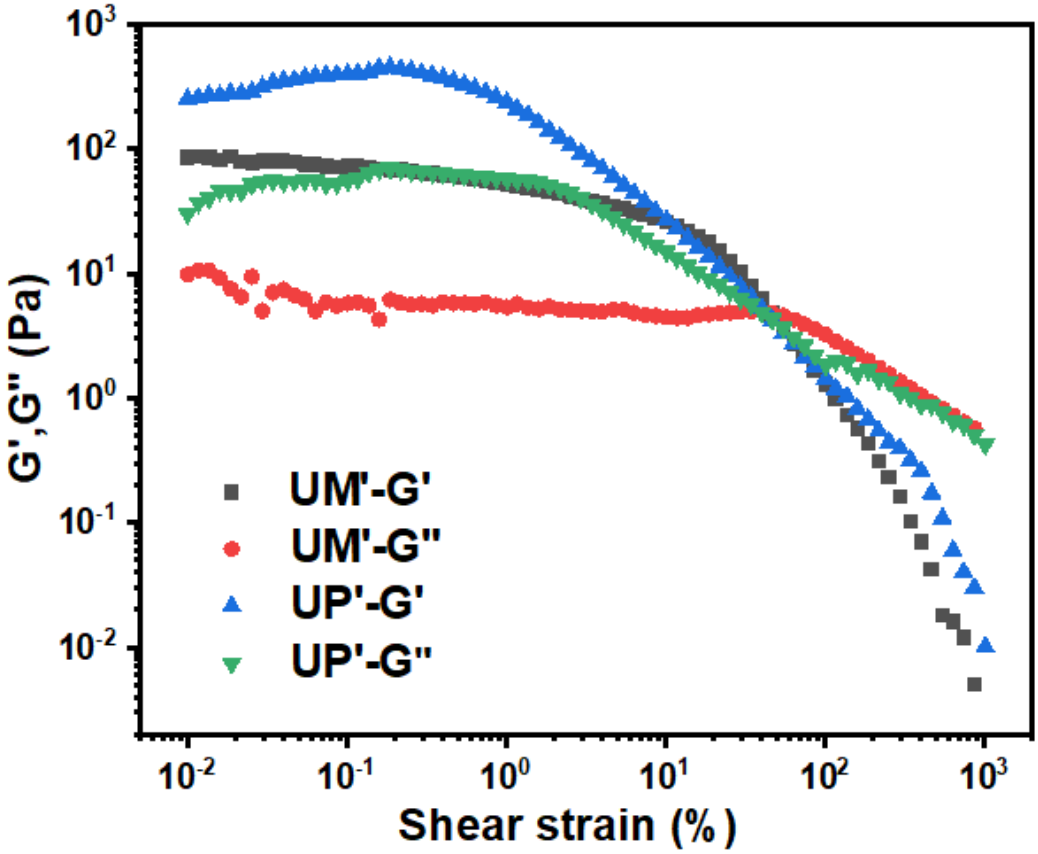

Figure S18. Storage moduli (G') and loss moduli (G'') of the Pickering emulsions (**UP'** concentration 8.33 mg/ml) stabilized by different MOF compounds (**UP'** and **UM'**) vs. % of shear strain rate. This is for oscillatory amplitude sweep, the frequency of the exciting sinusoidal signal (deformation) is kept constant at 1 Hz.

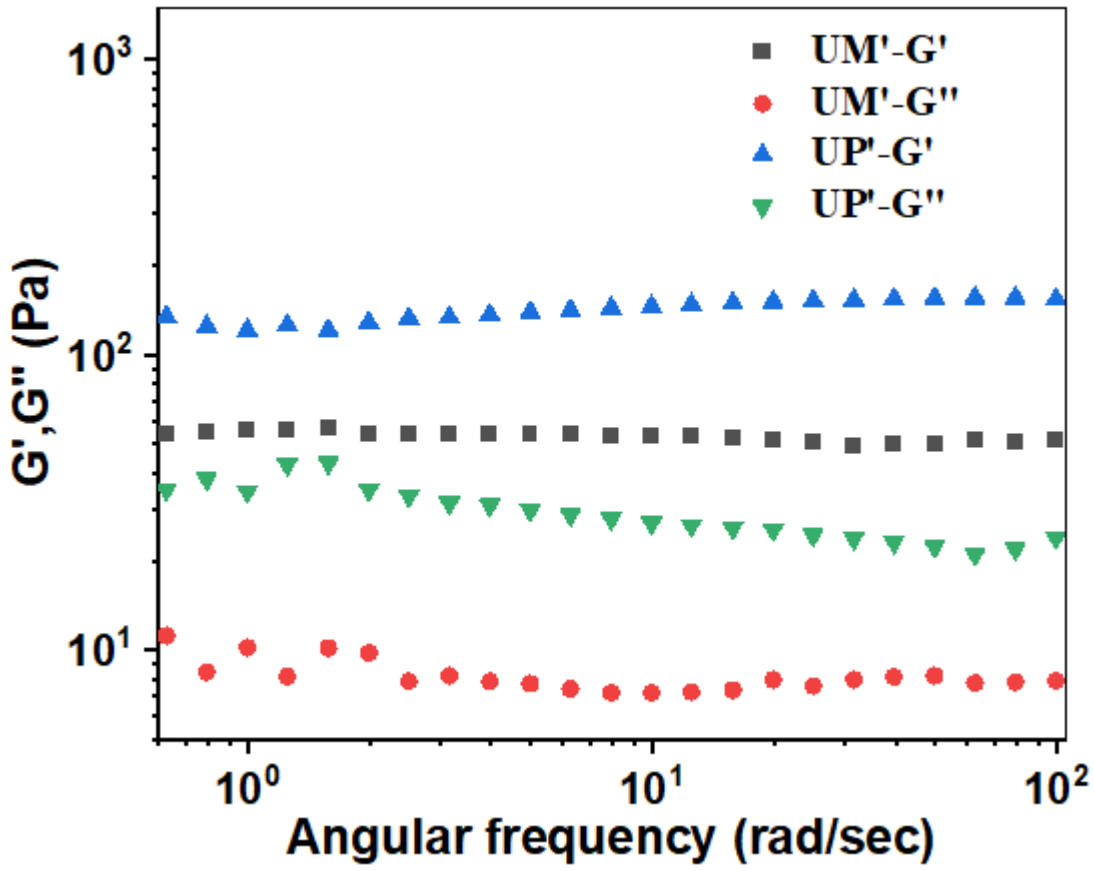

Figure S19. Storage moduli (G') and loss moduli (G'') of the Pickering emulsions (**UP'** concentration 8.33 mg/ml) stabilized by different MOF compounds (**UP'** and **UM'**) vs. angular frequency. This is oscillatory frequency sweep, where the amplitude of the sinusoidal excitation signal (deformation) is kept constant, while the frequency is varied gradually.

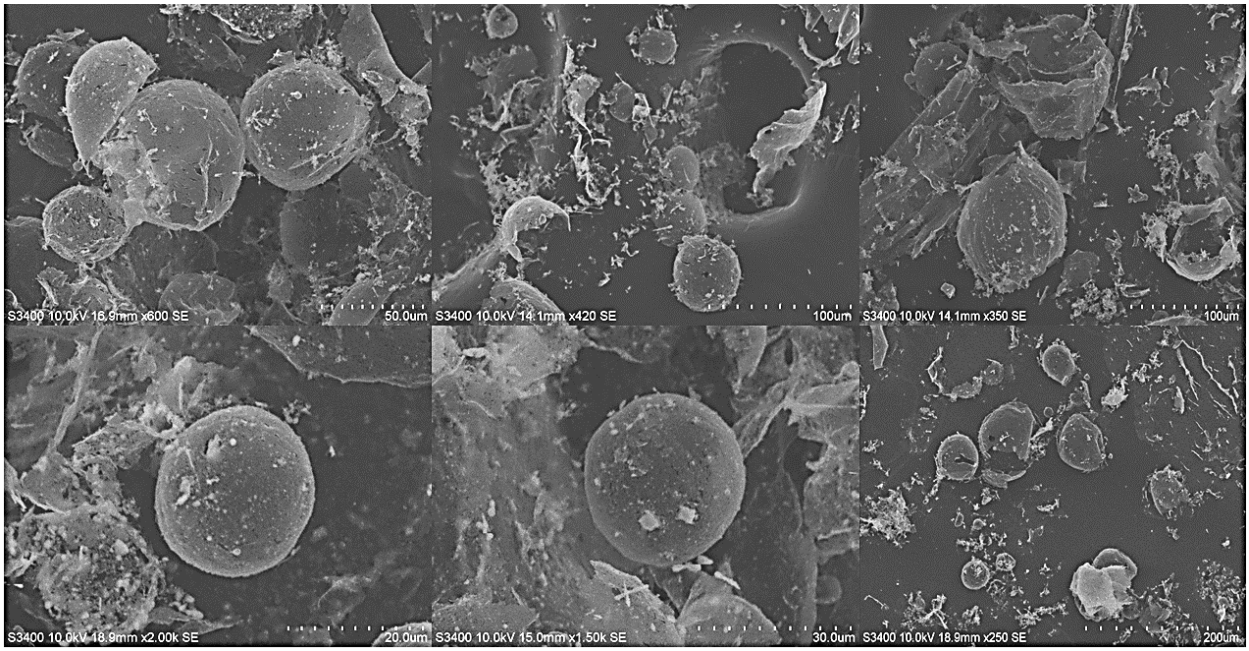

Figure S20. SEM images of round-shaped emulsion droplets stabilized by **UP'** (**UP'** concentration 8.33 mg/ml. Diameter of the round-shaped emulsion is ~50 μm). Scale bars are within each image.

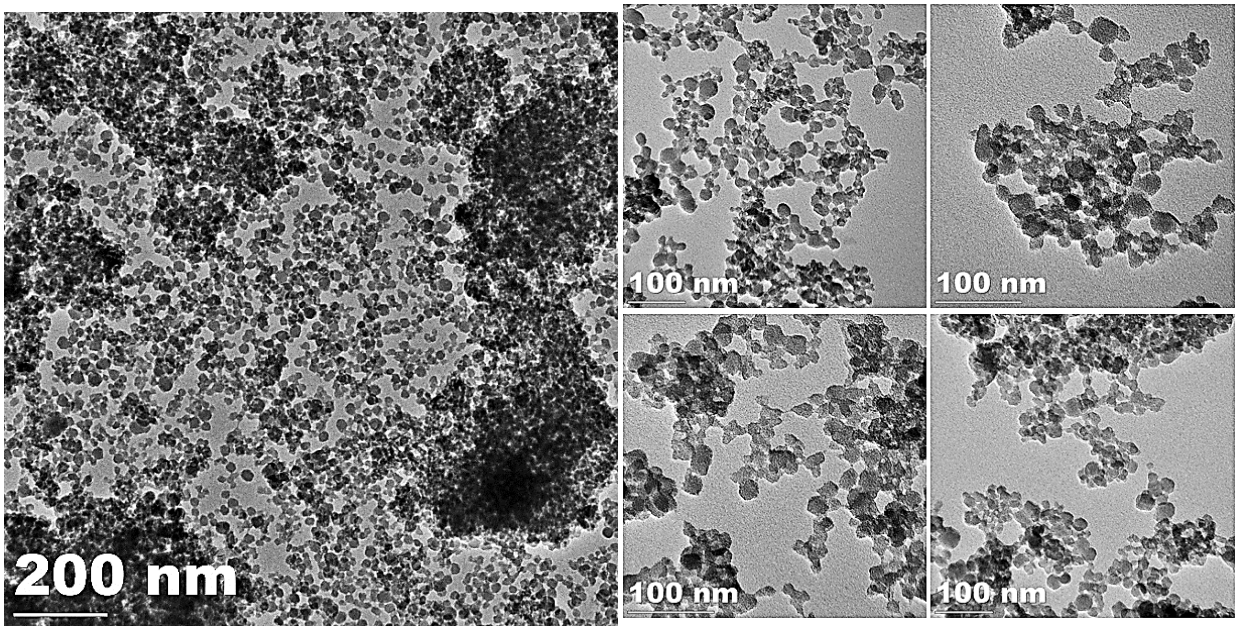

Figure S21. TEM images of Pickering emulsion stabilized by **UP'** (After freeze-drying). Scale bars are within each image.

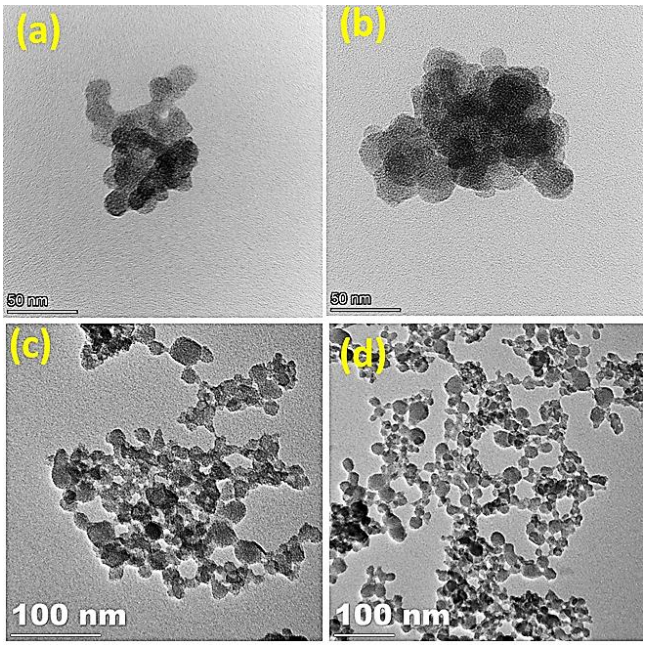

Figure S22. Comparison of size between particles of emulsion droplets (**UP'** concentration 8.33 mg/ml) and **UP'**: (a and b) TEM images of **UP'** before emulsion preparation. (c and d) TEM images of the Pickering emulsions stabilized by **UP'** (After freeze-drying).

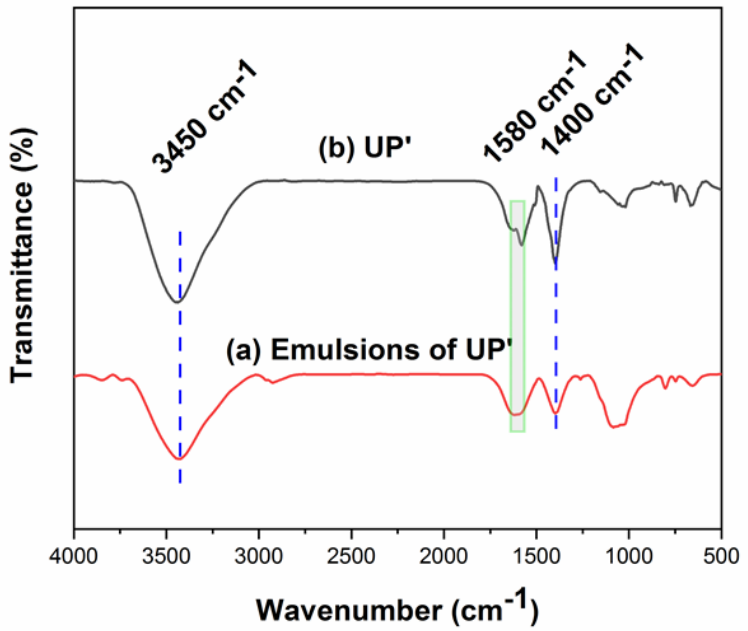

Figure S23. Comparison of FT-IR spectra between **UP'** (black) and dried emulsion (**UP'** concentration 8.33 mg/ml) droplet (red).

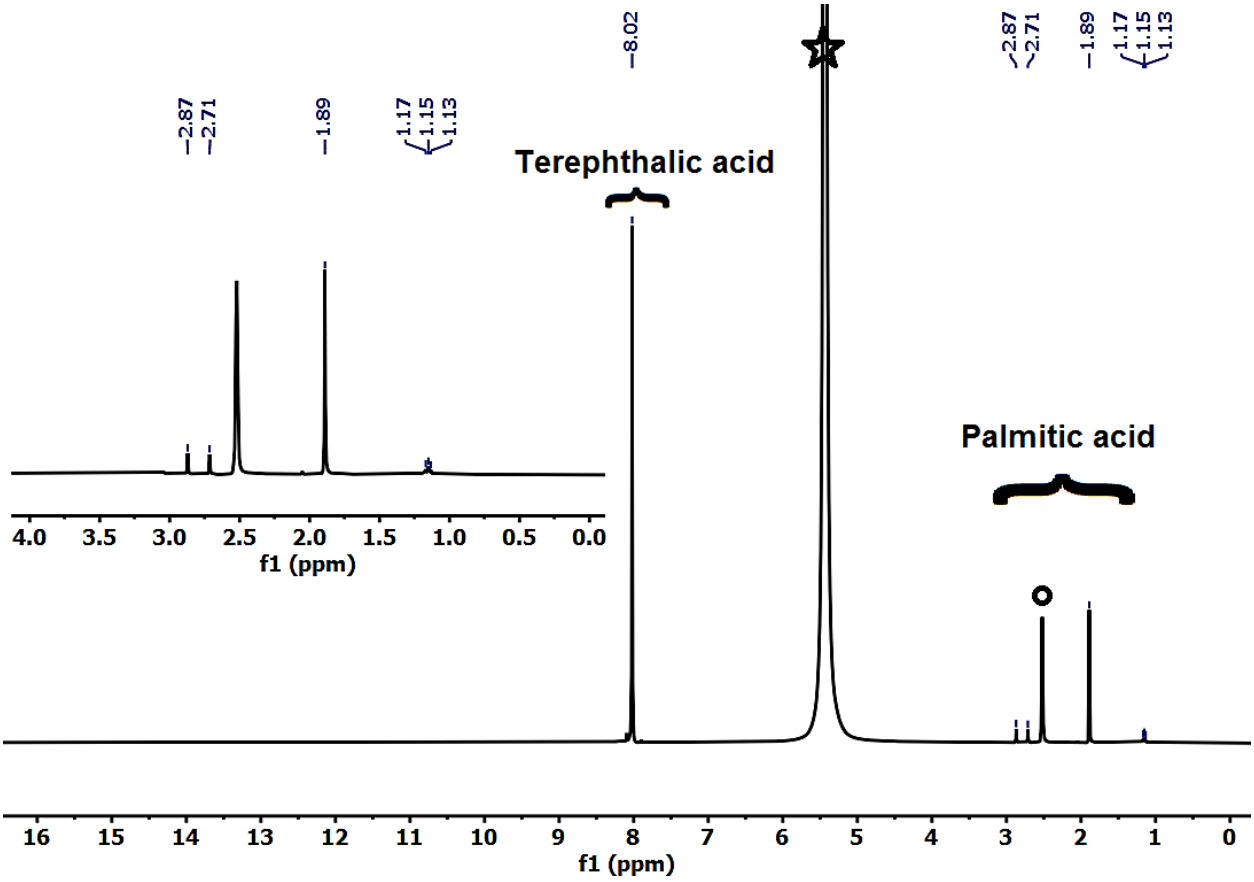

Figure S24. ^{1}H NMR spectra of dried emulsion (**UP'** concentration 8.33 mg/ml) droplet after digestion in HF/DMSO-d_6. The star represents the HF-H_2O, and circle denotes DMSO-d_6, respectively.

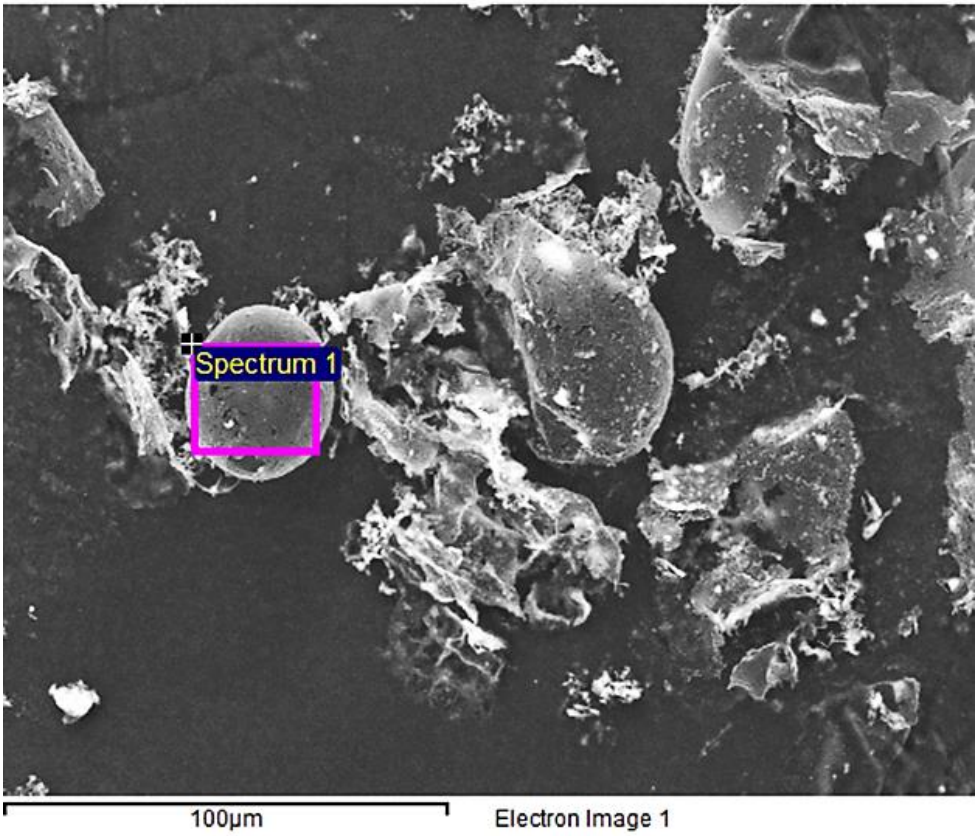

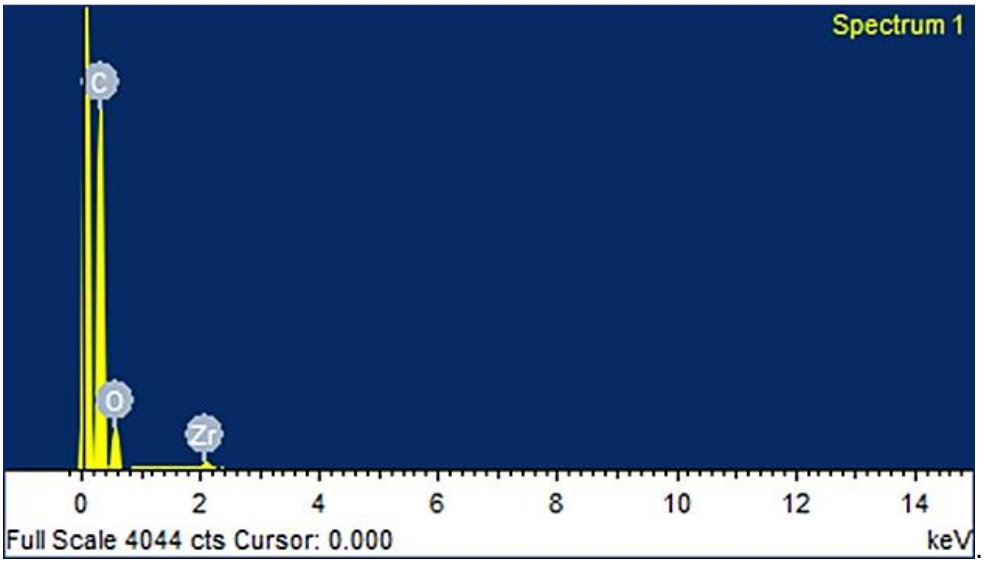

Figure S25. EDX spectrum of dried emulsion droplets stabilized by **UP'** (**UP'** concentration 8.33 mg/ml).

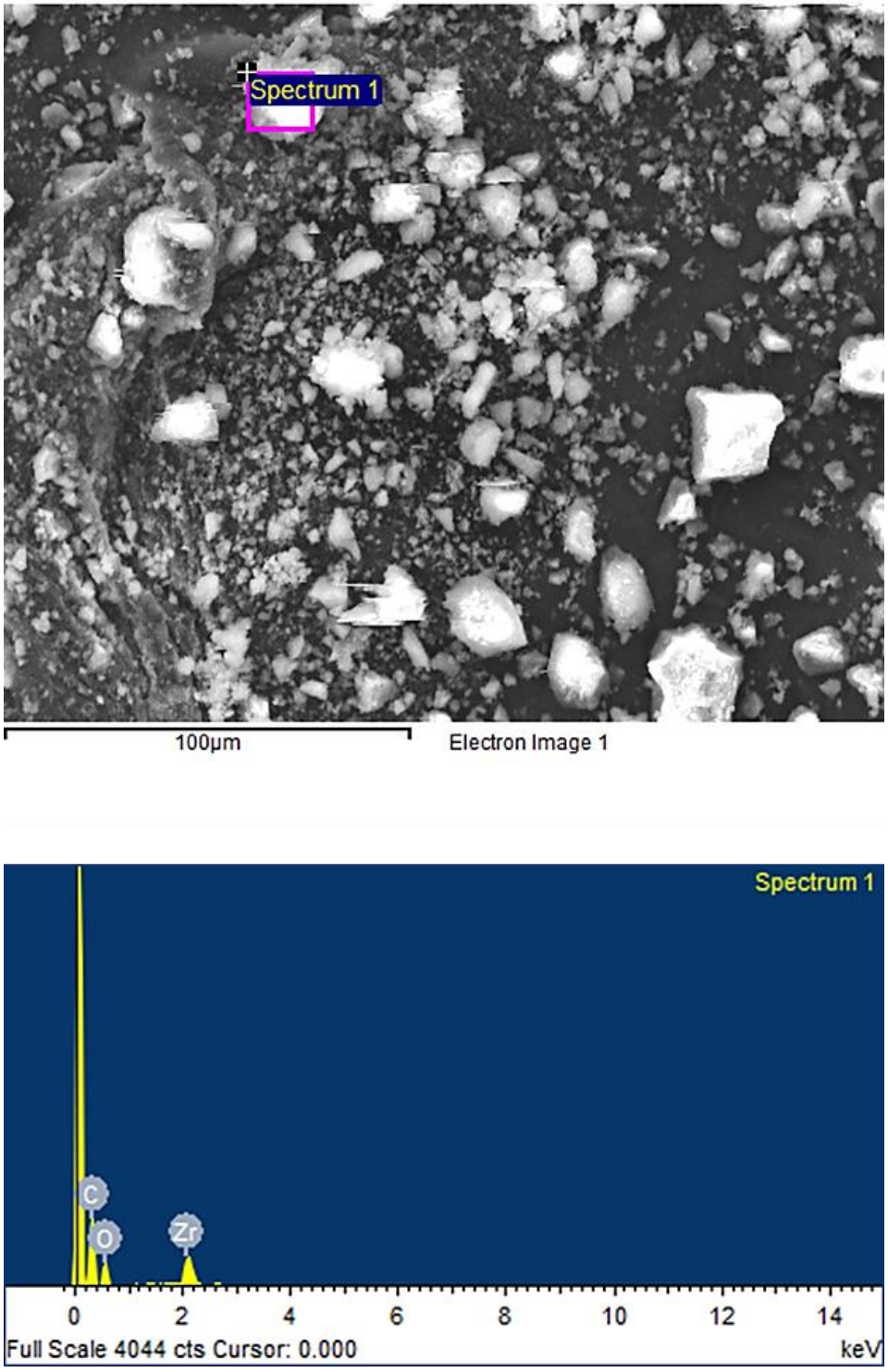

Figure S26. EDX spectrum of **UP'** (**UP'** concentration 8.33 mg/ml).

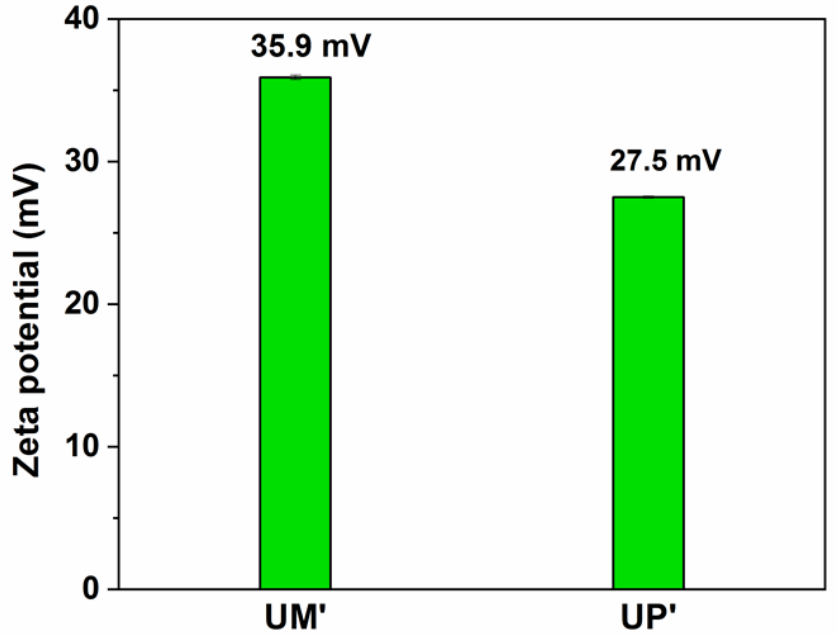

Figure S27. Zeta potential (ζ) of both **UP'** and **UM'** compounds (1 mg/ml in water) were measured at ambient temperature.

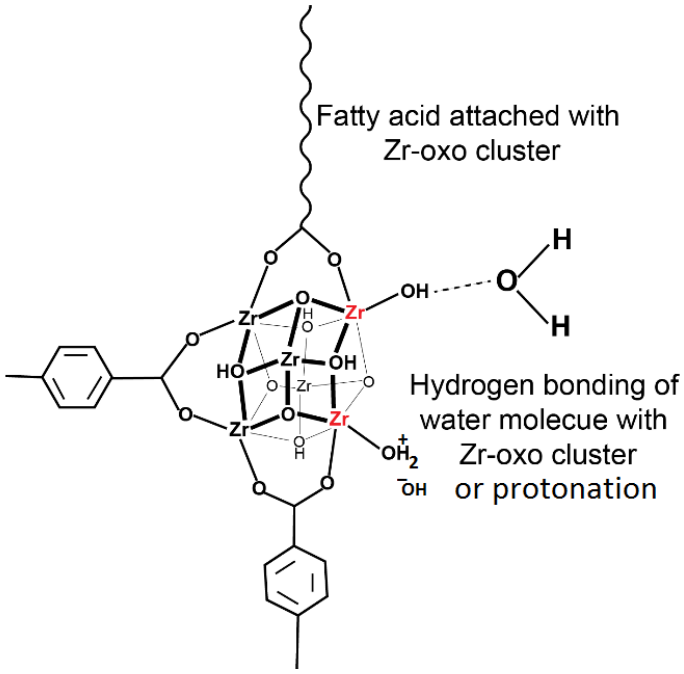

Figure S28. Illustration of cluster parts of the **UP'**: Water molecule interacts with Zr-oxo cluster, $[Zr_6(OH)_4(\mu_3\text{-}O)_4(\mathbf{L})_{6-x}]$, through H-bonding at the defect site (**L** = terephthalate and x = no. of missing linkers or no. of defects).

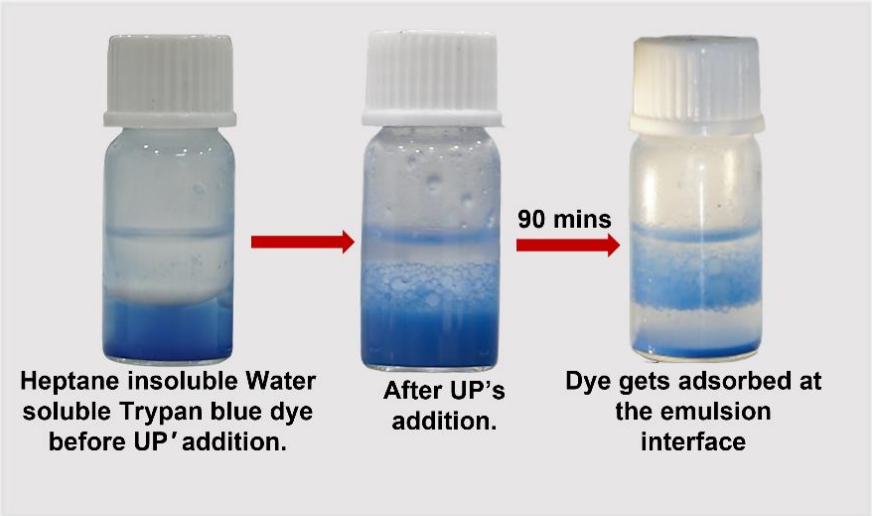

Figure S29. Series of images showing dye adsorption by emulsion. Initially, water-soluble Trypan blue bottom and clear upper n-heptane phase. After **UP'**s addition, emulsion starts forming. Finally, after 90 minutes of **UP'** addition, the blue-coloured dye get transferred to the emulsion phase.

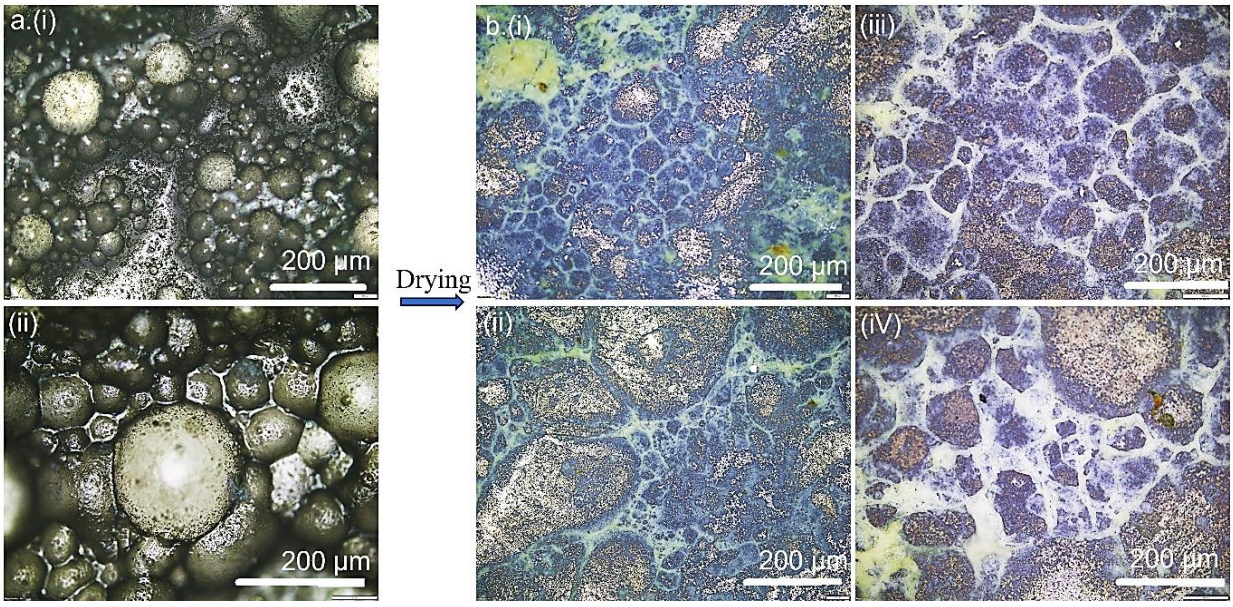

Figure S30. a.(i-ii) Optical microscopic images of **UP'** emulsion (**UP'** concentration 8.33 mg/ml) before drying. b.(i-iv) Continuous honeycomb pattern of leftover **UP'** particles after simple air drying of the same emulsion.

Table S1. Comparison of unit cell parameters of as-synthesized **UP** with reported UiO-66 MOF.

Compound name	**UP**	UiO-66[3]
Space group	$Fm\bar{3}m$	$Fm\bar{3}m$
Crystal system	Cubic	Cubic
a = b = c (Å)	20.790 (7)	20.7782 (7)
α = β = γ (°)	90	90
V (Å^3)	8986.0 (22)	8970.7 (5)
Radiation	Cu Kα_1	Cu Kα_1
Figure of merit (FOM)	35	-
R_{wp} (%)	5.51	6.4
R_p (%)	3.35	4.9

Table S2. Comparison of **A'** with other MOFs in the stabilization of Pickering emulsions.

SL. No.	MOFs or MOF-composites	Type of Pickering emulsions	Ref.
1	HKUST-1	Both water-in-oil and oil-in-water	[4]
2	ZIF-8@PS (PS = Poly-styrene)	Oil-in-water	[5]
3	Cu-BDC	Oil-in water	[6]
4	Cu-BDC/Poly(NMA)	CO_2-in-water	[7]
5	$Mn_3(BTC)_2$	CO_2-in-water	[8]
6	Ni-BDC	Ionic liquid-in-water and water-in-ionic liquid	[9]
7	MIL-96 (Al)	Oil-in-water	[10]
8	UiO-66/GO	Oil-in-water	[11]
9	UiO-66	Oil-in-water	[12]
10	UiO-66 and UiO-66-NH_2	Oil-in-water	[13]
11	**UP'**	Oil-in-water	This work

[a]Calculation of yield of the Synthesized MOF[2,14]:

$$6\ ZrOCl_2.\ 8H_2O + 6\ H_2BDC \rightarrow [Zr_6O_4(OH)_4\ (BDC)_6] \ +\ 12\ HCl\ +\ 46\ H_2O$$

The molecular formulation of UiO-66 MOF is $[Zr_6O_4(OH)_4\ (BDC)_6]$. So, the 6 moles of $ZrOCl_2.8H_2O$ (MW: 322.25 g mol^{-1}) will give one mole of $[Zr_6O_4(OH)_4\ (BDC)_6]$ (MW: 1664.06 g mol^{-1}), considering this, theoretical yield will be 86 mg. In our work, we obtained 38.7 mg of UiO-66 MOF (**UM'**) (Yield: 45%) when we used 100 mg of $ZrOCl_2.8H_2O$ and 50 mg of terephthalic acid. The same procedure was applied during the calculation of the yield of palmitic acid-connected UiO-66 MOF (**UP'**).

References

(1) Cavka, J. H.; Jakobsen, S.; Olsbye, U.; Guillou, N.; Lamberti, C.; Bordiga, S.; Lillerud, K. P. A New Zirconium Inorganic Building Brick Forming Metal Organic Frameworks with Exceptional Stability. *J. Am. Chem. Soc.* **2008**, *130*, 13850–13851.

(2) Shearer, G. C.; Chavan, S.; Bordiga, S.; Svelle, S.; Olsbye, U.; Lillerud, K. P. Defect Engineering: Tuning the Porosity and Composition of the Metal–Organic Framework UiO-66 via Modulated Synthesis. *Chem. Mater.* **2016**, *28*, 3749–3761.

(3) Zhu, L.; Zhang, D.; Xue, M.; Li, H.; Qiu, S. Direct Observations of the MOF (UiO-66) Structure by Transmission Electron Microscopy. *CrystEngComm* **2013**, *15*, 9356–9359.

(4) Xiao, B.; Yuan, Q.; Williams, R. A. Exceptional Function of Nanoporous Metal Organic Framework Particles in Emulsion Stabilisation. *Chem. Commun.* **2013**, *49*, 8208–8210.

(5) Huo, J.; Marcello, M.; Garai, A.; Bradshaw, D. MOF-Polymer Composite Microcapsules Derived from Pickering Emulsions. *Adv. Mater.* **2013**, *25*, 2717–2722.

(6) Song, P.; Natale, G.; Wang, J.; Bond, T.; Hejazi, H.; Siegler, H. de la H.; Gates, I.; Lu, Q. 2D and 3D Metal–Organic Framework at the Oil/Water Interface: A Case Study of Copper Benzenedicarboxylate. *Adv. Mater. Interf.* **2019**, *6*, 1801139.

(7) Yang, Z.; Cao, L.; Li, J.; Lin, J.; Wang, J. Facile Synthesis of Cu-BDC/Poly(N-Methylol Acrylamide) HIPE Monoliths via CO2-in-Water Emulsion Stabilized by Metal-Organic Framework. *Polymer (Guildf).* **2018**, *153*, 17–23.

(8) Liu, C.; Zhang, J.; Zheng, L.; Zhang, J.; Sang, X.; Kang, X.; Zhang, B.; Luo, T.; Tan, X.; Han, B. Metal–Organic Framework for Emulsifying Carbon Dioxide and Water. *Angew. Chem. Int. Ed.* **2016**, *55*, 11372–11376.

(9) Li, Z.; Zhang, J.; Luo, T.; Tan, X.; Liu, C.; Sang, X.; Ma, X.; Han, B.; Yang, G. High Internal Ionic Liquid Phase Emulsion Stabilized by Metal–Organic Frameworks. *Soft Matter* **2016**, *12*, 8841–8846.

(10) Lorignon, F.; Gossard, A.; Carboni, M.; Meyer, D. Microstructural and Rheological Investigation of Upcycled Metal-Organic Frameworks Stabilized Pickering Emulsions. *J. Colloid Interface Sci.* **2021**, *586*, 305–314.

(11) Zhang, F.; Liu, L.; Tan, X.; Sang, X.; Zhang, J.; Liu, C.; Zhang, B.; Han, B.; Yang, G. Pickering Emulsions Stabilized by a Metal–Organic Framework (MOF) and Graphene Oxide (GO) for Producing MOF/GO Composites. *Soft Matter* **2017**, *13*, 7365–7370.

(12) Zhu, H.; Zhang, Q.; Zhu, S. Assembly of a Metal–Organic Framework into 3 D Hierarchical Porous Monoliths Using a Pickering High Internal Phase Emulsion Template. *Chem. Eur. J.* **2016**, *22*, 8751–8755.

(13) Ma, P.; Zhang, J.; Teng, Z.; Zhang, Y.; Bauchan, G. R.; Luo, Y.; Liu, D.; Wang, Q. Metal–Organic Framework-Stabilized High Internal Phase Pickering Emulsions Based on Computer Simulation for Curcumin Encapsulation: Comprehensive Characterization and Stability Mechanism. *ACS Omega* **2021**, *6*, 26556–26565.

(14) Shearer, G. C.; Chavan, S.; Ethiraj, J.; Vitillo, J. G.; Svelle, S.; Olsbye, U.; Lamberti, C.; Bordiga, S.; Lillerud, K. P. Tuned to Perfection: Ironing Out the Defects in Metal–Organic Framework UiO-66. *Chem. Mater.* **2014**, *26*, 4068–4071.